

# RSC Advances



This is an *Accepted Manuscript*, which has been through the Royal Society of Chemistry peer review process and has been accepted for publication.

*Accepted Manuscripts* are published online shortly after acceptance, before technical editing, formatting and proof reading. Using this free service, authors can make their results available to the community, in citable form, before we publish the edited article. This *Accepted Manuscript* will be replaced by the edited, formatted and paginated article as soon as this is available.

You can find more information about *Accepted Manuscripts* in the [Information for Authors](#).

Please note that technical editing may introduce minor changes to the text and/or graphics, which may alter content. The journal's standard [Terms & Conditions](#) and the [Ethical guidelines](#) still apply. In no event shall the Royal Society of Chemistry be held responsible for any errors or omissions in this *Accepted Manuscript* or any consequences arising from the use of any information it contains.

1 **Continuously Tuning the Spectral Response of Chiral Plasmonic Patchy Particles through**  
2 **Galvanic Replacement Reaction**

3  
4 *George K. Larsen, Nicholas Stom, and Yiping Zhao*

5  
6 Department of Physics and Astronomy, and Nanoscale Science and Engineering Center,  
7 University of Georgia, Athens, GA 30602

8  
9 \*Email: georgelarsen@physast.uga.edu; Phone: +1-706-542-6230; Fax: +1-706-542-2492  
10  
11  
12

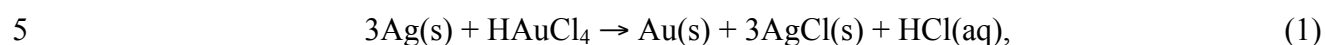
13 **Abstract:** We demonstrate the continuous tuning of the circular dichroism spectra of chiral  
14 patchy particle structures fabricated by dynamic shadowing growth (DSG) using the galvanic  
15 replacement reaction (GRR), which is a wet chemical process where Au ions in solution are  
16 gradually replaced by Ag atoms in a support. It is found that the unpolarized and circular  
17 polarization optical responses generally shift to longer wavelengths as a function of reaction  
18 time. The red-shifts in the spectra are attributed to changes in the ambient refractive index, chiral  
19 patch morphology, and material composition. For reaction times less than 4 minutes, the circular  
20 dichroism spectra can be adjusted over a wide range of wavelengths in the visible and near-  
21 infrared region with only slight reductions in magnitude. Thus, the combination of dry (DSG)  
22 and wet (GRR) nanofabrication techniques offers a route to dynamically tune the spectral  
23 response of chiral plasmonic thin films.

24 **Keywords:** chiral plasmonics; dynamic shadowing growth; glancing angle deposition; colloid  
25 monolayers; wet chemistry  
26  
27

1 From ancient dichroic glass to medieval stained glass to modern theranostic tools, people have  
2 long employed the remarkable plasmonic properties of noble metal nanoparticles.<sup>1</sup> In spite of this  
3 extensive history, new developments continue to emerge from the fertile field of plasmonics.  
4 For example, metal nanoparticles that exhibit chirality (*i.e.*, lack reflective symmetry) have been  
5 the focus of many recent works and have garnered much attention.<sup>2</sup> This interest in chiral  
6 plasmonic nanoparticles and thin films has been incited by Pendry's proposal that negative  
7 refraction can be achieved for one handedness of circular polarization for strongly chiral films,  
8 even if both the permittivity and permeability values are positive over the region of interest.<sup>3</sup> In  
9 addition to negative refraction, chiral plasmonic materials have shown great promise for optical  
10 filtering and biosensing.<sup>4-8</sup> Much progress has also been made in the fabrication of chiral metal  
11 nanostructures, and many different methods have been described in the literature that meet this  
12 challenge.<sup>2</sup> These fabrication methods can be generally grouped into either wet chemistry  
13 techniques (*e.g.*, chiral molecule modification,<sup>9</sup> biomolecular self-assembly,<sup>10</sup> and gyroid block  
14 copolymer self-assembly<sup>11</sup>) and dry micro-/nanotechnology (*e.g.*, electron beam lithography,<sup>12</sup>  
15 photolithography,<sup>4</sup> Si etching,<sup>13</sup> and dynamic shadowing growth (DSG)<sup>14, 15</sup>). While different  
16 techniques have their own unique advantages and disadvantages, dry nanotechnology methods  
17 generally produce films with greater circular anisotropy.<sup>12, 16</sup> DSG, in particular, has  
18 demonstrated the ability to create strongly chiral films with high throughput.<sup>17-20</sup> However, wet  
19 chemistry and dry nanotechnology processes are not mutually exclusive, and their combination  
20 could allow for additional modification and optimization of the different chiral structures not  
21 achievable through a single process.

22 The galvanic replacement reaction (GRR) is an interesting wet chemical process that is a  
23 simple and efficient way to gradually replace Au ions in a solution with Ag atoms from a

1 support.<sup>21</sup> While the GRR for Au replacing Ag is the best known, GRRs are a broad class of  
2 reactions, and the mechanism behind these spontaneous reactions is always due to a difference in  
3 redox potentials. More specifically, the specific GRR for Au replacing Ag happens according to  
4 the following equation:<sup>22</sup>



6 where the standard reduction potential versus the standard hydrogen electrode is 0.22 V for the  
7 AgCl/Ag pair and 0.99 V for AuCl<sub>4</sub><sup>-</sup>/Au. This difference between the reduction potentials drives  
8 the oxidation of the template material (Ag) by the metal (Au) salt precursor. This single-step  
9 spontaneous electroless deposition process is a well-known method and has been  
10 comprehensively studied.<sup>23</sup> Sun and Xia have established that GRR proceeds through two  
11 different processes:<sup>24</sup> (1) the Ag template is dissolved as Au atoms deposit epitaxially on the  
12 surface of the template to form a seamless, hollow nanostructure with an outer boundary  
13 composed of Au/Ag alloy; (2) a dealloying process selectively removes Ag atoms from the  
14 alloyed walls, leaving a porous network of Au. Thus, the GRR offers a simple route to modify  
15 Ag nanostructures to variously create bimetallic Ag/Au structures, porous Ag/Au bimetallic  
16 structures, and porous pure Au nanostructures, where the different type of structure achieved  
17 depends on the reaction parameters (time, concentrations, etc.). This offers a potential method to  
18 tune the plasmonic properties of noble metal nanostructures by varying the material composition  
19 and morphology. Furthermore, such bimetallic structures can exhibit unique properties not  
20 found in single material nanostructures, including enhanced activity of plasmonic resonances.<sup>25</sup>  
21 From the discussion above, it is clear that chiral plasmonic nanostructures fabricated using dry  
22 nanotechnology methods could benefit from the application of the Au/Ag GRR, yet no such  
23 study has been performed. Therefore, we have applied the Au/Ag GRR (reaction equation 1) to

1 the chiral patchy particle structure fabricated using DSG, and monitored the optical response as a  
2 function of reaction time using transmission ellipsometry.<sup>5</sup> It is found that the unpolarized and  
3 circular polarization responses are generally red-shifted as a function of reaction time, which is a  
4 result of AgCl deposition. For reaction times less than 4 minutes, the circular dichroism spectra  
5 can be adjusted over a wide range of wavelengths in the visible and near-infrared region with  
6 only slight reductions in magnitude. Thus, GRR offers a route to dynamically tune the spectral  
7 response of chiral plasmonic thin films in the visible region.

8         The fabrication process for the Ag chiral patchy films begins by creating self-assembled  
9 colloid monolayers (SACMs) of polystyrene nanospheres (Polysciences, diameter of 500 nm) on  
10 glass and Si substrates. The SACMs are loaded into a vacuum deposition system such that their  
11 surface normal and the vapor incident direction form an oblique polar angle,  $\theta = 86^\circ$ . Ag (Kurt  
12 J. Lesker, 99.999%) is then deposited in 30 nm increments at azimuthal angles,  $\varphi = 0^\circ, 120^\circ$ , and  
13  $240^\circ$  sequentially, until a desired thickness of 120 nm at each  $\varphi$  is achieved. More detailed  
14 information regarding the fabrication of chiral patchy particles can be found in previous works.<sup>14,</sup>  
15 <sup>17</sup> It is important to note that the quality of the obtained chiral patchy particles is directly related  
16 to the quality of the SACM used as a template. However, significant advances in SACM  
17 fabrication have been made, making colloidal self-assembly a large-scale, high throughput  
18 technique.<sup>26</sup> The SACM fabrication technique employed here creates consistently aligned arrays  
19 on the centimeter scale, which allows for the creation uniform chiral patchy particles over the  
20 entire film size ( $\sim 1 \text{ cm}^2$ ). GRR is performed by first completely immersing each of the as-  
21 deposited Ag chiral patchy films into separate Eppendorf tubes containing 1 mL of 0.1 mM  
22 chloroaurate acid solution ( $\text{HAuCl}_4 \cdot 3\text{H}_2\text{O}$ , 99.999%, Sigma-Aldrich). The chiral patchy particle  
23 substrates are immersed in solution for pre-determined times, corresponding with a total

1 immersion time of  $t = 1$  s, 30 s, 1 min, 2 min, 3 min, 4 min, 5 min, 7 min, 10 min, 15 min, and 20  
2 min, respectively. After removing from the test tubes at a specific time, each sample is rinsed  
3 thoroughly by DI water, dried in a  $N_2$  stream, measured by ellipsometry, and then either re-  
4 immersed for further treatments and measurements or set aside for morphological  
5 characterization. The beam size diameter of the ellipsometer is  $\sim 2$  mm and is smaller than the  
6 array size, so each ellipsometry measurement contains the optical responses of  $\sim 10^{10}$  chiral  
7 patchy particles.

8         The CD spectra for a chiral patchy particle film for different GRR times,  $t$ , at various  
9 increments over 20 minutes are shown in **Figure 1a**. It is important to note that the CD spectra  
10 are obtained through a Mueller matrix ellipsometry method that separates the linear and circular  
11 polarization contributions, as well as the birefringent from the dichroic contributions.<sup>5</sup> The  
12 chiral patchy particle film is a single domain structure, and therefore, the CD response is initially  
13 very strong, showing several resonances and convoluted bisignate features. As  $t$  proceeds, these  
14 features generally decrease in intensity and red-shift, and after  $t = 10$  minutes, a significant  
15 reduction in intensity is observed. No significant changes are observed in the spectra over the  $t$   
16 = 15 – 20 minute period. Notably, the negative peak that is initially around  $\lambda \approx 700$  nm, Peak 1,  
17 red-shifts by more than 250 nm during the GRR process, and after only  $t = 4$  minutes, it has  
18 already shifted to near  $\lambda = 900$  nm (**Figure 1b**). Furthermore, the intensity of this peak does not  
19 significantly change over the range  $t = 0.5 - 4$  minutes (**Figure 1c**), and over this same period,  
20 the peak shifts from  $\lambda \approx 700 - 900$  nm. On the other hand, Peak 2 does not significantly change  
21 its spectral location over the GRR, hovering around  $\lambda \approx 520$  nm, yet its intensity follows the  
22 same pattern as Peak 1 and does not significantly change over the range  $t = 0.5 - 4$  minutes.  
23 These observations demonstrate that the GRR method offers a route to dynamically tune the CD

1 response of chiral plasmonic structures over a large portion of the visible and near-infrared  
2 region.

3         The behavior of the CD spectra during GRR is also echoed in the unpolarized  
4 transmittance spectra, as shown in **Figure 2a**. Initially several resonances can be observed as  
5 dips in the transmission spectra, and these transmission dips also generally flatten and red-shift  
6 as the GRR proceeds. Further, two significant dips appear around  $\lambda \approx 700$  nm and  $\lambda \approx 500$  nm at  
7  $t = 0$ , and are labeled as Dip 1 and Dip 2 since they correspond with the aforementioned Peaks 1  
8 and 2, respectively. In comparing the wavelength shifts of Dip 1 from the transmittance  
9 spectrum with Peak 1 from the CD spectrum (**Figure 2b**) as functions of  $t$ , it is found that the  
10 shifts are identical. This resonance generating Dip 1 is attributed to the localized surface  
11 plasmon resonances (LSPRs) of the noble metal nanostructures. Therefore, the shifts in the  
12 transmittances and corresponding CD spectra induced by the GRR acting on the plasmonic  
13 structures could arise from two different effects: an increase in nanostructure volume or a change  
14 in the refractive index of the material or ambient. It is important to note that the observed dips  
15 (extinction) in the transmittance spectra could have some contributions from scattering since the  
16 sizes of the patchy particles are on the order of the incident wavelengths. However, a recent  
17 investigation using finite-difference-time-domain simulations has determined that the extremely  
18 strong local circular dichroism in these patchy particles arises from the difference between the  
19 coupling of right and left-handed circular polarized light with the plasmonic modes of the chiral  
20 metal patches.<sup>27</sup> Thus, while some scattering may occur, the CD spectra of the pristine chiral  
21 patchy particles originate from plasmonic modes in the silver coating, and the energies of these  
22 modes change as the GRR proceeds.

1 In order to better understand the morphological changes in the Ag chiral patchy particles  
2 during the GRR, SEM images are taken at various stages during the reaction process. **Figure 3**  
3 shows the micrographs for  $t = 0, 1.5, 20$  minutes. There appears to be a slight increase in  
4 porosity and surface roughness of the structures after  $t = 1.5$  minutes. After  $t = 20$  minutes, the  
5 patchy coating is significantly rougher and more porous, and some of the patches have been  
6 pulled off of the polystyrene beads. Additionally, new crystal structures appear on the surface of  
7 the film. Interestingly, these crystals interact strongly with the electron beam of the microscope,  
8 and change from well-defined cubic and rectangular structures to globular, amorphous structures  
9 after a few seconds of electron beam irradiation (**Figure 3d**). Image analysis software (ImageJ)  
10 can be employed to quantify the morphological changes observed in the SEM images, and it is  
11 found that the average area of the chiral patches,  $a_{avg}$ , increases as a function of GRR time. For  $t$   
12  $= 0, 1.5,$  and  $20$  minutes it was found that  $a_{avg} = 94 \pm 7 \text{ nm}^2, 101 \pm 8 \text{ nm}^2,$  and  $130 \pm 90 \text{ nm}^2,$   
13 respectively. Thus, the particle sizes increase with increasing GRR time, a factor that could  
14 contribute to the red-shifting of the CD and transmittance spectra.

15 Energy-dispersive X-ray spectroscopy (EDX) measurements are performed in order to  
16 confirm the composition of the patchy particles during the GRR process. Interestingly, the EDX  
17 spectra are virtually identical over the  $t = 0.5 - 20$  minute time period, showing only the presence  
18 of Ag and Cl within the large background of C and Si (from the SACM substrates). Thus, X-ray  
19 diffraction (XRD) measurements are also used to determine the crystalline composition of the  
20 patchy particles. As expected, the chiral patchy particles show a polycrystalline Ag diffraction  
21 pattern at  $t = 0$  (**Figure 4**). However, after  $t = 20$  minutes, new peaks emerge that correspond  
22 with the diffraction pattern of AgCl. Thus, it is highly likely that the new crystals seen in the  
23 SEM images at  $t = 20$  minutes (**Figure 3c**) are AgCl that are produced during the reaction. The



1 known reversible photochromic decomposition of AgCl could be related to the morphological  
2 changes seen in (**Figure 3d**). It is important to note that the XRD measurements are not able to  
3 detect the presence of Au in this case since the diffraction peaks of Au are completely  
4 overlapped by the peaks of Ag. It does appear that the GRR reaction occurs as described in  
5 **Equation 1** given the presence of AgCl in significant enough amounts to be detected by XRD.  
6 That is, Ag from the chiral patchy coatings is being consumed to create AgCl. However, it does  
7 not appear that the Au epitaxially replaces Ag within the patches during the GRR process,  
8 especially since EDX does not provide direct evidence for the presence of Au on the surface of  
9 the films. While it is not clear why Au does not deposit epitaxially in this case, it is suspected  
10 that the surface roughness of the deposited Ag and the presence of the polystyrene nanospheres  
11 might play a role in the abnormal behavior of the Au atoms in this structure.<sup>28,29</sup> In any case, the  
12 deposition of AgCl on the chiral patches should contribute to the red-shifting of the CD and  
13 transmittance spectra by increasing the ambient refractive index surrounding the plasmonic  
14 nanostructures. The magnitude of this shift is related to the optical and morphological properties  
15 of both the plasmonic nanoparticle and adsorbing AgCl, in addition to the actual amount of AgCl  
16 deposited.

17 In conclusion, chiral patchy particle films have been modified by the Au/Ag galvanic  
18 replacement reaction. The reaction induces morphological changes in the Ag patchy coatings by  
19 increasing the surface roughness and particle size, creating additional pores, and depositing AgCl  
20 on the surfaces, and these changes modify the chiral LSPRs of the chiral patches. While Au or  
21 Au/Ag alloy are not detected in meaningful quantities, the GRR significantly modifies the CD  
22 spectra of the chiral patchy films in a very short time period. In general, the CD intensity  
23 decreases and the spectral features red-shift. Notably though, a negative peak shifts from  $\lambda \approx$

1 700 – 900 nm over the reaction times  $t = 0.5 - 4$  minutes, without a change in magnitude. Thus,  
2 as desired, the GRR method does dynamically modify the CD response of the chiral patchy  
3 particles over a wide range of wavelengths in the visible and near-infrared region. These results  
4 demonstrate that the combination of DSG for chiral structure fabrication, coupled with wet  
5 chemical methods, such as GRR, offers significant freedom and potential in the design of chiral  
6 plasmonic structures for specific applications.

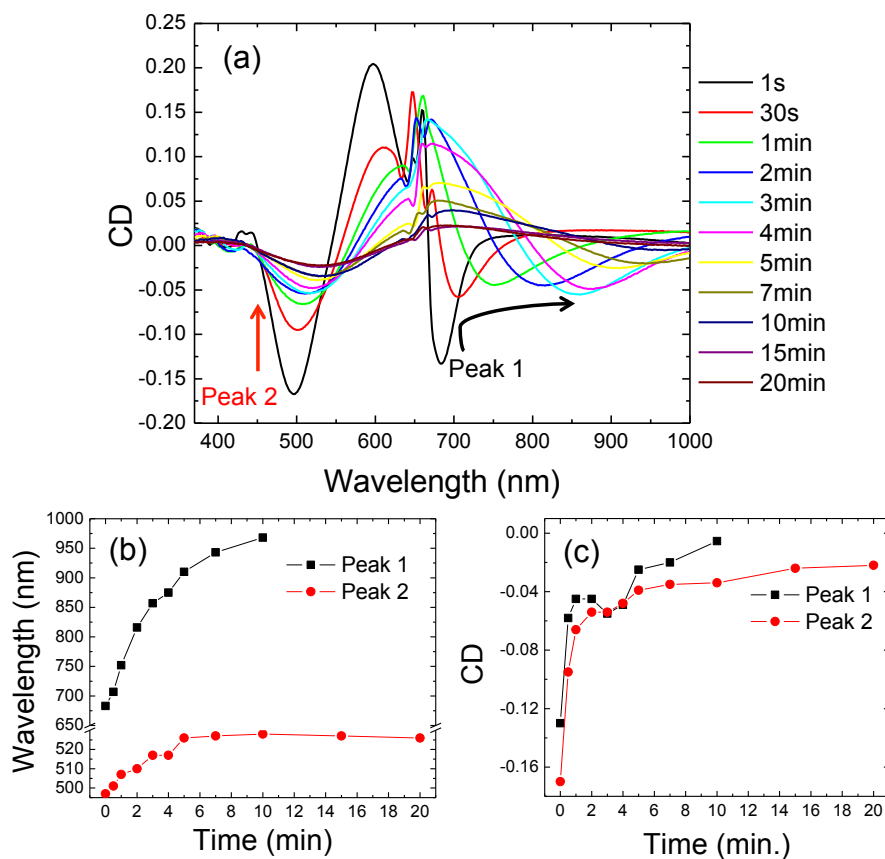
### 7 **Acknowledgement**

8 We gratefully acknowledge support from the National Science Foundation (Grant No. ECCS-  
9 1029609 and CMMI-1435309).

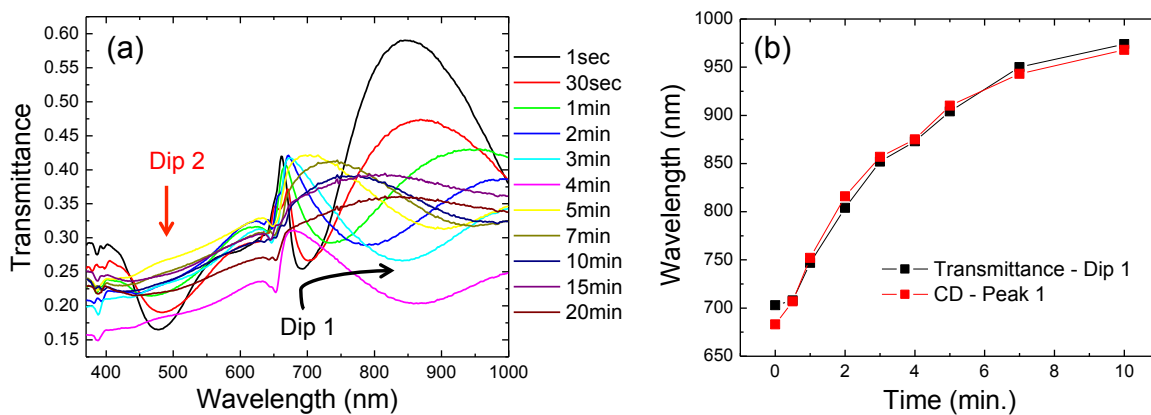
1 **References:**

- 2 1. S. A. Maier, M. L. Brongersma, P. G. Kik, S. Meltzer, A. A. Requicha and H. A.  
3 Atwater, *Adv. Mater.*, 2001, **13**, 1501-1505.
- 4 2. V. K. Valev, J. J. Baumberg, C. Sibilica and T. Verbiest, *Adv. Mater.*, 2013, **25**, 2517-  
5 2534.
- 6 3. J. B. Pendry, *Science*, 2004, **306**, 1353-1355.
- 7 4. J. K. Gansel, M. Latzel, A. Frölich, J. Kaschke, M. Thiel and M. Wegener, *Appl. Phys.*  
8 *Lett.*, 2012, **100**, 101109.
- 9 5. G. K. Larsen and Y. Zhao, *Appl. Phys. Lett.*, 2014, **105**, 071109.
- 10 6. E. Hendry, T. Carpy, J. Johnston, M. Popland, R. Mikhaylovskiy, A. Laphorn, S. Kelly,  
11 L. Barron, N. Gadegaard and M. Kadodwala, *Nat. Nanotechnol.*, 2010, **5**, 783-787.
- 12 7. W. Ma, H. Kuang, L. Xu, L. Ding, C. Xu, L. Wang and N. A. Kotov, *Nat. Commun.*,  
13 2013, **4**.
- 14 8. J. K. Gansel, M. Thiel, M. S. Rill, M. Decker, K. Bade, V. Saile, G. von Freymann, S.  
15 Linden and M. Wegener, *Science*, 2009, **325**, 1513-1515.
- 16 9. A. O. Govorov, Z. Fan, P. Hernandez, J. M. Slocik and R. R. Naik, *Nano Lett.*, 2010, **10**,  
17 1374-1382.
- 18 10. A. Kuzyk, R. Schreiber, Z. Fan, G. Pardatscher, E.-M. Roller, A. Hogege, F. C. Simmel,  
19 A. O. Govorov and T. Liedl, *Nature*, 2012, **483**, 311-314.
- 20 11. K. Hur, Y. Francescato, V. Giannini, S. A. Maier, R. G. Hennig and U. Wiesner, *Angew.*  
21 *Chem.*, 2011, **123**, 12191-12195.
- 22 12. C. Helgert, E. Pshenay-Severin, M. Falkner, C. Menzel, C. Rockstuhl, E. B. Kley, A.  
23 Tunnermann, F. Lederer and T. Pertsch, *Nano Lett.*, 2011, **11**, 4400-4404.
- 24 13. K. M. McPeak, C. D. van Engers, M. Blome, J. H. Park, S. Burger, M. A. Gosálvez, A.  
25 Faridi, Y. R. Ries, A. Sahu and D. J. Norris, *Nano Lett.*, 2014, **14**, 2934-2940.
- 26 14. G. Larsen, Y. He, W. Ingram, E. LaPaquette, J. Wang and Y. Zhao, *Nanoscale*, 2014, **6**,  
27 9467-9476.
- 28 15. J. G. Gibbs, A. G. Mark, T.-C. Lee, S. Eslami, D. Schamel and P. Fischer, *Nanoscale*,  
29 2014, **6**, 9457-9466.
- 30 16. A. G. Mark, J. G. Gibbs, T. C. Lee and P. Fischer, *Nat. Mater.*, 2013, **12**, 802-807.
- 31 17. G. Larsen, Y. He, W. Ingram and Y. Zhao, *Nano Lett.*, 2013, **13**, 6228-6232.

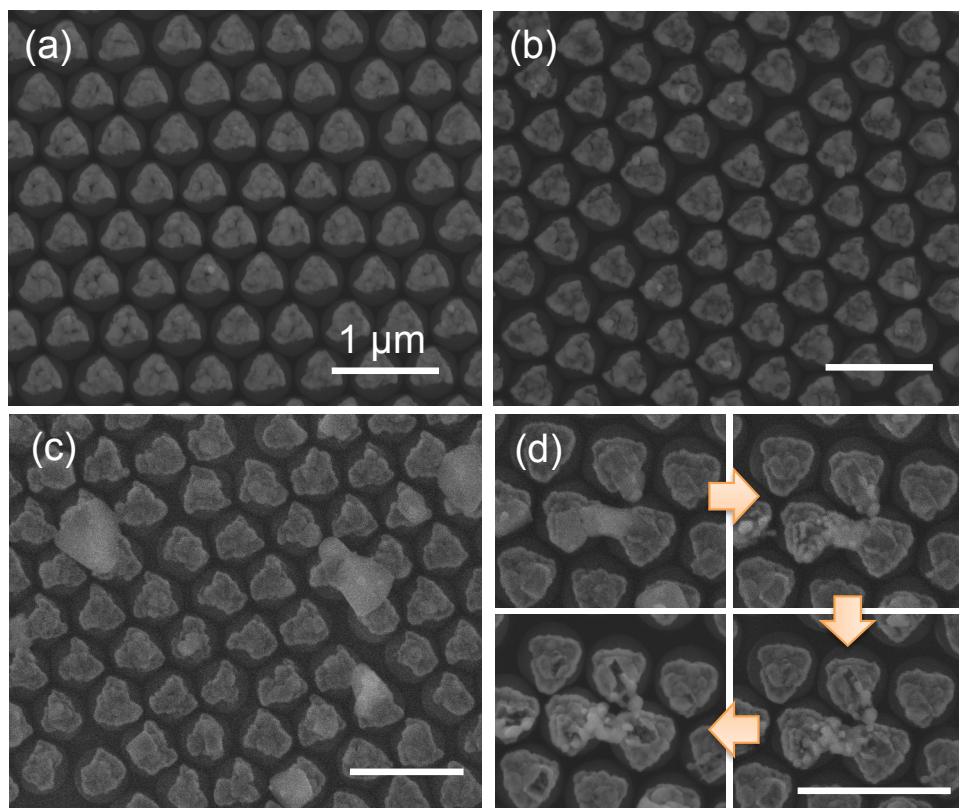
- 1 18. G. K. Larsen, Y. He, J. Wang and Y. Zhao, *Adv. Opt. Mater.*, 2014, **2**, 245-249.
- 2 19. Y. He, G. K. Larsen, W. Ingram and Y. Zhao, *Nano Lett.*, 2014, **14**, 1976-1981.
- 3 20. Y. He, G. Larsen, X. Li, W. Ingram, F. Chen and Y. Zhao, *Adv. Opt. Mater.*, 2015.
- 4 21. C. M. Cobley and Y. Xia, *Mater. Sci. Eng., R*, 2010, **70**, 44-62.
- 5 22. Y. Sun and Y. Xia, *Science*, 2002, **298**, 2176-2179.
- 6 23. C. Song, J. L. Abell, Y. He, S. H. Murph, Y. Cui and Y. Zhao, *J. Mater. Chem.*, 2012, **22**,  
7 1150-1159.
- 8 24. Y. Sun and Y. Xia, *J. Am. Chem. Soc.*, 2004, **126**, 3892-3901.
- 9 25. M. B. Cortie and A. M. McDonagh, *Chem. Rev.*, 2011, **111**, 3713-3735.
- 10 26. P. Gao, J. He, S. Zhou, X. Yang, S. Li, J. Sheng, D. Wang, T. Yu, J. Ye and Y. Cui, *Nano*  
11 *Lett.*, 2015, **15**, 4591-4598.
- 12 27. Y. He, K. Lawrence, W. Ingram and Y. Zhao, *ACS Photonics*, 2015, **2**, 1246-1252.
- 13 28. C.-P. Chang, C.-C. Tseng, J.-L. Ou, W.-H. Hwu and M.-D. Ger, *Colloid Polym. Sci.*,  
14 2010, **288**, 395-403.
- 15 29. W. Cai, W. Wang, L. Lu and T. Chen, *Colloid Polym. Sci.*, 2013, **291**, 2023-2029.
- 16  
17  
18



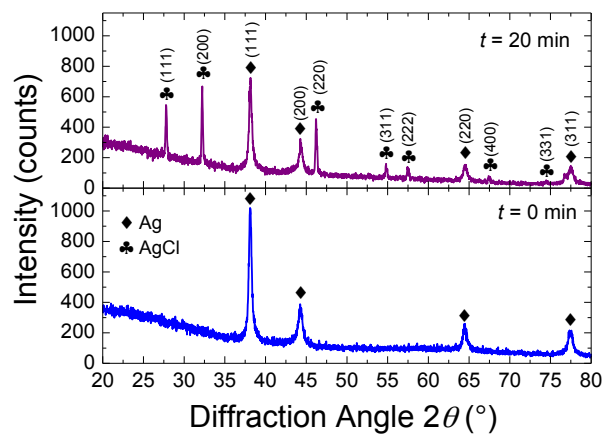
**Figure 1.** (a) CD spectra of the chiral patchy particles for various GRR reaction times,  $t$ . (b) wavelength and (c) CD intensity shifts of Peak 1 and Peak 2.



**Figure 2.** (a) Transmittance spectra for various GRR reaction times,  $t$ . (b) Comparison between the wavelength shifts of transmittance Dip 1 and CD Peak 1.



**Figure 3.** (a)-(c) SEM images of the chiral patchy particles at GRR times,  $t = 0$ , 1.5, and 20 minutes, respectively. (d) Sequential SEM images showing the effect of electron radiation on the surface crystals.

1  
2  
3  
4  
5  
6  
7  
8  
9  
10  
11  
12  
13  
14  
15  
16  
17  
18  
19  
20  
21  
22

**Figure 4.** XRD patterns of the chiral patchy particle films at GRR reaction times  $t = 0$  and  $t = 20$  minutes. Peak attributions for Ag and AgCl are from card numbers 00-004-0783 and 00-31-1238, respectively.



- 1 **TOC entry:** We demonstrate the continuous tuning of the circular dichroism spectra of chiral
- 2 patchy particle arrays using the galvanic replacement reaction.

